FOUNDATIONS
ADVANCES

ISSN: 2053-2733
journals.iucr.org/a

On the determination of dense coincidence site lattice planes

Adam Morawiec

Acta Cryst. (2022). A**78**, 491–497

FOUNDATIONS ADVANCES

ISSN 2053-2733

On the determination of dense coincidence site lattice planes

Adam Morawiec*

Institute of Metallurgy and Materials Science, Polish Academy of Sciences, Reymonta 25, Krakow, 30-059, Poland. *Correspondence e-mail: nmmorawi@cyf-kr.edu.pl

Received 28 February 2022
Accepted 4 September 2022

Edited by S. J. L. Billinge, Columbia University, USA

Keywords: crystal lattice; coincidence site lattice; intercrystalline interface; Hermite normal form; Niggli reduction.

Supporting information: this article has supporting information at journals.iucr.org/a

The concept of coincidence site lattice (CSL) is used in descriptions of geometry of some intercrystalline boundaries. In face-centered cubic and body-centered cubic metals, atoms are located at the nodes of lattices, and results concerning lattice nodes are applicable to atomic sites. One of the criteria for special boundary configurations is that the boundary passes through a plane with a high density of coinciding atomic sites. Hence, there is an issue of identification of such planes. This paper describes a simple and reliable method for determining the planes with high densities of coinciding lattice nodes. The key elements of the procedure are the Hermite normal form of an integer matrix and Niggli reduction of the CSL basis. In its general form, the method is applicable to arbitrary three-dimensional lattices possessing a common three-dimensional sublattice. The densest and second-densest planes are determined for low-Σ CSLs of cubic lattices.

1. Introduction

The notion of coincidence site lattice (CSL) or the intersection of two interpenetrating lattices is used in the description of geometry of interfaces between crystallites. The CSL model is applied mainly to homophase interfaces (grain boundaries). Real grain boundaries are affected by many factors (*e.g.* impurity segregation), but even if the additional complications are excluded, the low energy of boundaries cannot be explained by purely geometric models (Sutton & Balluffi, 1987). On the other hand, geometric models play a significant role as skeletons supporting physically more realistic approaches. CSLs and special boundaries play the role of reference points in the space of possible boundary geometries.

The term 'site' in CSL is unfortunate as it can be associated with an atomic site (Gratias & Portier, 1982), whereas the CSL concerns coinciding lattice nodes. The text below can be read with CSL interpreted as the abbreviation for 'common sublattice'. Clearly, the atomic coincidence at the boundary is physically more meaningful than the coincidence of lattices. However, in the important case of elemental face-centered cubic (f.c.c.) and body-centered cubic (b.c.c.) metals, atoms are located at the nodes of *cF*- and *cI*-type lattices, respectively. In effect, results concerning coinciding lattices are applicable to atomic sites.

CSLs are three-dimensional objects, whereas interfaces are two-dimensional. A simple geometric premise for a special two-dimensional configuration is that a boundary plane has a high planar density of coinciding atomic sites. Thus, assuming a CSL misorientation between two lattices, there is a question about lattice planes with a high density of common nodes. In other words, one looks for planes of CSLs with small areas of

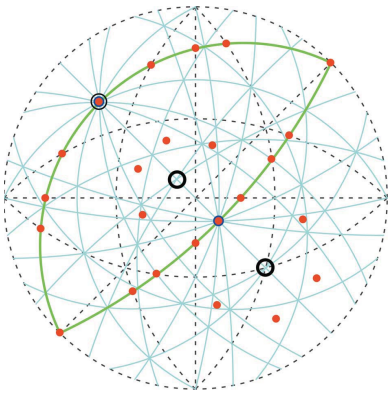

planar cells. The subject has been discussed in numerous articles, and methods of determining the planes have been considered (see, *e.g.*, Brandon *et al.*, 1964; Chalmers & Gleiter, 1971; Goodhew *et al.*, 1978; Wolf, 1992; Acton & Bevis, 1971; Smith, 1974; Yang, 1982). However, data and results concerning the planes with a high density of common nodes are not always correct.

This paper describes a simple and reliable method for determining the planes with high densities of coinciding lattice nodes. The method is applied to coinciding cubic lattices, and the densest and second-densest planes are listed for high-coincidence misorientations. At the end, the method is generalized to arbitrary, possibly different, three-dimensional lattices having a common three-dimensional sublattice.

While Sutton & Balluffi (1987) concluded that the planar density of coinciding atomic sites in a grain boundary is not related to boundary properties, the idea persists in the literature. The amount of current grain boundary data far exceeds that available at the time of publication of Sutton & Balluffi (1987), so the results presented below will make it possible to compare recent grain boundary measurements with correct theoretical planar densities.

2. The method

It is assumed below that the intersection or common sublattice of two three-dimensional lattices Λ and Λ' is itself a three-dimensional lattice. It will be denoted by $\Lambda \cap \Lambda'$. The index of a sublattice is defined as the ratio of the volumes of primitive cells of the sublattice and the lattice. A CSL is partly characterized by its indices Σ and Σ' with respect to the lattices Λ and Λ', respectively. In the case of homophase boundaries, the second lattice is obtained by rotating the first one, *i.e.* $\Lambda' = R\Lambda$, where R denotes the rotation. Clearly, in this case, $\Sigma' = \Sigma$.

The lattice reciprocal to Λ is denoted by Λ^*. It is well known that if L is a sublattice of Λ, then Λ^* is a sublattice of L^*, and the indices of L in Λ and Λ^* in L^* are equal. This implies that $(\Lambda \cap \Lambda')^*$ is the smallest-cell superlattice of both Λ^* and Λ'^*, or in symbols, $(\Lambda \cap \Lambda')^* = \Lambda^* \cup \Lambda'^*$. Thus, the intersection $\Lambda \cap \Lambda' = (\Lambda^* \cup \Lambda'^*)^*$ can be derived from the lattice $\Lambda^* \cup \Lambda'^*$ generated by vectors of Λ^* and Λ'^*.

The standard method for determining a lattice basis from a set of generating vectors is by using the Hermite normal form (HNF) of an integer matrix (*e.g.* Cohen, 1993, p. 73). With the generating vectors being basis vectors of two lattices, HNF gives a basis of the smallest-cell superlattice of the lattices. Having lattices Λ and Λ', one can get Λ^* and Λ'^*, use the HNF-based method to determine $\Lambda^* \cup \Lambda'^*$, and then the relationship $\Lambda \cap \Lambda' = (\Lambda^* \cup \Lambda'^*)^*$ to obtain the intersection of Λ and Λ'.

The goal is to get planes of lattices Λ and Λ' dense with common nodes. They are also planes of the CSL; as such, these are planes with small areas of their planar cells. The lattice planes with the smallest areas of cells are based on short vectors of the CSL. Thus, knowing the CSL, one needs to get its shortest vectors and simple linear combinations thereof, and see which of these relevant vectors span the smallest cell. A method for getting the shortest vectors of a lattice is called lattice (or basis or cell) reduction. Well known in crystallography is the Niggli-reduction procedure.

In brief, the method of determination of the densest lattice planes described below is practically based on two computational tools: the HNF of an integer matrix and Niggli reduction of the lattice basis. Algorithms for both HNF and Niggli reduction are easily accessible – see, *e.g.*, Cohen (1993) and Křivý & Gruber (1976), respectively. With these two elements, determination of the densest lattice planes is straightforward.

2.1. Hermite normal form

All one needs here is the case of integer 3×6 rank-3 matrices with matrix columns containing vector components. An integer matrix in HNF has the shape

$$[\mathbf{0}\ \mathbf{0}\ \mathbf{0}\ H] = \begin{bmatrix} 0 & 0 & 0 & \star & \star & \star \\ 0 & 0 & 0 & 0 & \star & \star \\ 0 & 0 & 0 & 0 & 0 & \star \end{bmatrix},$$

where the square matrix H is upper triangular and its entries satisfy the conditions $H_{ii} > H_{ij} \geq 0$ for $j > i$. The columns preceding H have only zero entries. For an arbitrary integer matrix M of full rank, there exists a unimodular integer matrix U such that the matrix $MU = \mathrm{HNF}(M)$ is in HNF. Every integer matrix of full row rank has a unique HNF. Reduction of a matrix to its HNF can be seen as the determination of a basis of a lattice generated by columns of the matrix. The formula $M = \mathrm{HNF}(M)U^{-1}$ is nothing other than a way of expressing columns of M via linear combinations of the columns of $\mathrm{HNF}(M)$.

Based on the HNF of integer matrices, one can define Hermite reduced form of a rational matrix M; it is given by $m^{-1}\mathrm{HNF}(mM)$, where m is the least common multiple of denominators of the entries of M. The 3×3 matrix obtained by dropping the first three (*i.e.* zero) columns of the 3×6 matrix $m^{-1}\mathrm{HNF}(mM)$ will be denoted by $\mathrm{HR}(M)$.

2.2. Niggli reduction

The Niggli reduction of the lattice basis is a classic tool of crystallography. The Niggli-reduced basis consists of the shortest non-coplanar vectors of the lattice. The basis satisfies conditions which make the basis unique (apart from its handedness and orientation). A set of conditions for Niggli reduction is given, *e.g.*, by Křivý & Gruber (1976). The Niggli reduction also provides Niggli character and Bravais type of the lattice (de Wolff, 2005). With basis vectors $\mathbf{b}_i$ ($i = 1, 2, 3$) represented as columns of the matrix $[\mathbf{b}_1\,\mathbf{b}_2\,\mathbf{b}_3] = [\mathbf{b}_i]$, the matrix with vectors resulting from Niggli reduction of $[\mathbf{b}_i]$ will be denoted by $\mathrm{NR}([\mathbf{b}_i])$. With $\mathrm{NR}([\mathbf{b}_i]) = [\mathbf{c}_i]$, the magnitudes of the vectors $\mathbf{c}_i$ satisfy the inequalities $|\mathbf{c}_1| \leq |\mathbf{c}_2| \leq |\mathbf{c}_3|$.

2.3. Steps of the procedure

With known bases $[\mathbf{a}_i]$ and $[\mathbf{a}'_i]$ of CSL-related lattices Λ and Λ', the steps leading to determination of the plane with the largest density of common lattice nodes are as follows:

1. Compute the reciprocals $[\mathbf{a}_i^*] = ([\mathbf{a}_i]^{-1})^{\mathrm{T}} = [\mathbf{a}_i]^{-\mathrm{T}}$ and $[\mathbf{a}_i'^*] = [\mathbf{a}_i']^{-\mathrm{T}}$, *i.e.* bases of Λ^* and Λ'^*.

2. Using HNF, get the basis $[\mathbf{b}_i^*]$ of the lattice generated by the vectors $\mathbf{a}_i^*$ and $\mathbf{a}_i'^*$; $[\mathbf{b}_i^*]$ is a basis of $\Lambda^* \cup \Lambda'^*$.

3. Get $[\mathbf{b}_i] = [\mathbf{b}_i^*]^{-\mathrm{T}}$ reciprocal to $[\mathbf{b}_i^*]$; due to $(\Lambda^* \cup \Lambda'^*)^* = \Lambda \cap \Lambda'$, the matrix $[\mathbf{b}_i]$ comprises a basis of the common sublattice $\Lambda \cap \Lambda'$.

4. Reduce the basis $[\mathbf{b}_i]$; the Niggli-reduced basis, say $[\mathbf{c}_i]$, consists of the shortest vectors of the CSL.

5. Using the vectors $\mathbf{c}_i$ of the reduced basis, get pairs of relevant vectors spanning two-dimensional lattices with small areas of cells.

6. Determine the pair of relevant vectors corresponding to the smallest area.

7. The two-dimensional lattice spanned by that pair is a lattice plane in both Λ and Λ'; get its Miller indices in the bases of these two lattices or in conventional bases. The resulting plane has the largest planar density of common lattice nodes. With a sufficiently large set of relevant vectors one can also determine the second-densest plane. The above scheme can be easily translated into a computer algorithm.

In the case of CSL-related cubic lattices Λ and $\Lambda' = R\Lambda$, the basis vectors $\mathbf{a}_i$ and $\mathbf{a}_i'$ have rational components in the conventional orthogonal basis. Hence, also entries of the matrix $M = [\mathbf{a}_1^*\ \mathbf{a}_2^*\ \mathbf{a}_3^*\ \mathbf{a}_1'^*\ \mathbf{a}_2'^*\ \mathbf{a}_3'^*]$ are rational, *i.e.* M is in the domain of the HR mapping, and the key steps

$$[\mathbf{b}_i^*] = \mathrm{HR}(M) \quad \text{and} \quad [\mathbf{c}_i] = \mathrm{NR}([\mathbf{b}_i])$$

are directly applicable. The rest of the procedure is just computation of basis reciprocals and dealing with the relevant vectors.

2.4. Relevant vectors

The Niggli reduction provides the shortest non-coplanar lattice vectors $\mathbf{c}_i$ ($i = 1, 2, 3$). Pairs of these vectors span planar cells with relatively small areas. The area of the cell spanned by two vectors is equal to the magnitude of the vector product of these vectors. To get the densest plane, it is enough to consider the four pairs $(\mathbf{c}_1, \mathbf{c}_2)$, $(\mathbf{c}_2, \mathbf{c}_3)$, $(\mathbf{c}_3, \mathbf{c}_1)$ and $(\mathbf{c}_1, \mathbf{c}_2 + \mathbf{c}_3)$. More combinations are needed to determine the second-densest plane. To obtain the results listed below, the considered relevant vectors had the form

$$\sum_{i=1}^{3} n_i \mathbf{c}_i$$

with $n_i = -1, 0$ or $+1$ and $\sum |n_i| \neq 0$. Since the area spanned by $\mathbf{a}$ and $\mathbf{b}$ is equal to that spanned by $\mathbf{a}$ and $-\mathbf{b}$, only one of two vectors with opposite signs needs to be taken into account. This gives $(3^3 - 1)/2 = 13$ relevant vectors. It is easy to verify that there are up to 25 distinct non-zero areas of cells spanned by the relevant vectors. The pair of relevant vectors spanning the smallest area is a basis of the sought-after densest CSL plane.

In the cubic case, with vectors given in the conventional orthogonal basis, the vector product of vectors spanning a lattice plane has components proportional to Miller indices of that plane.

Table 1
Misorientation parameters of CSLs of cubic lattices for $\Sigma \leq 33$.

With the parameter k provided in the second column, the exact smallest misorientation angle is $\omega = \arccos(k/(2\Sigma))$. The axes of rotations representing the misorientations are given in the conventional orthogonal reference frame. All presented results for cubic lattices and $\Sigma \leq 33$ rely on misorientation parameters fixed at values listed in this table.

Σ	k	ω (°)	Axis
3	3	60.0000	[111]
5	8	36.8699	[100]
7	11	38.2132	[111]
9	14	38.9424	[110]
11	14	50.4788	[110]
13*a*	24	22.6199	[100]
13*b*	23	27.7958	[111]
15	20	48.1897	[210]
17*a*	30	28.0725	[100]
17*b*	16	61.9275	[221]
19*a*	34	26.5254	[110]
19*b*	26	46.8264	[111]
21*a*	39	21.7868	[111]
21*b*	30	44.4153	[211]
23	35	40.4591	[311]
25*a*	48	16.2602	[100]
25*b*	31	51.6839	[331]
27*a*	46	31.5863	[110]
27*b*	44	35.4309	[210]
29*a*	42	43.6028	[100]
29*b*	40	46.3972	[221]
31*a*	59	17.8966	[111]
31*b*	38	52.2003	[211]
33*a*	62	20.0500	[110]
33*b*	55	33.5573	[311]
33*c*	34	58.9924	[110]

2.5. Indices of planes

In general, a vector $\mathbf{v}$ perpendicular to a plane common to the lattices Λ and Λ' is parallel to the vectors $\sum_i h_i \mathbf{a}_i^*$ and $\sum_i h_i' \mathbf{a}_i'^*$, where $(h_1\ h_2\ h_3) = (h\ k\ l)$ and $(h'_1\ h'_2\ h'_3) = (h'\ k'\ l')$ are coprime Miller indices of the plane in Λ and Λ', respectively. The indices can be computed from $\mathbf{v}$ using

$$h_i \propto \mathbf{v} \cdot \mathbf{a}_i \quad \text{and} \quad h_i' \propto \mathbf{v} \cdot \mathbf{a}_i', \tag{1}$$

and they are mutually related via $h_j' = -\sum_i h_i (\mathbf{a}_i^* \cdot \mathbf{a}_j')$. The $-$ sign arises by assuming that a vector representing a boundary of a crystal points outward from the crystal.

In the case of cubic lattices related by $\Lambda' = R\Lambda$, when indices are in reference to the conventional orthogonal basis, both $[\mathbf{a}_j]$ and $[\mathbf{a}_j^*]$ are proportional to identity matrices, and based on $\mathbf{a}_i' = R\mathbf{a}_i$, one has $h_j' = -\sum_i h_i R_{ij}$, where R_{ij} is the ijth entry of the orthogonal matrix representing R.

2.6. Equivalent boundary parameters

One additional issue which needs to be taken into account is that planes with different Miller indices but the same density of CSL nodes may be symmetrically equivalent. Detailed description of equivalences between boundary parameters is beyond the scope of this paper. However, it is worth noting that the equivalences are a consequence of point symmetries

of crystals and grain exchange symmetry. The general scheme for getting equivalent boundary parameters involves both lattice misorientations and interface planes in a coordinated manner (Morawiec, 2009). However, in the proposed procedure, the misorientation parameters are fixed. Thus, only the symmetry operations changing the parameters of the interface plane but leaving the misorientation parameters unchanged need to be considered. In the cubic case and $m\bar{3}m$ point-group symmetry, symmetrically equivalent representations of a boundary can be easily identified.

One needs to stress again the impact of grain exchange symmetry. For instance, one may consider two planes which arise as the densest for *cF* lattices related by Σ7; their indices given in the form $(h\ k\ l) \parallel (h'\ k'\ l')$ are $(\bar{3}\,\bar{5}\,1) \parallel (5\,3\,\bar{1})$ and $(\bar{1}\,3\,5) \parallel (1\,\bar{5}\,\bar{3})$. These boundaries are equivalent only if the grain exchange symmetry is assumed.

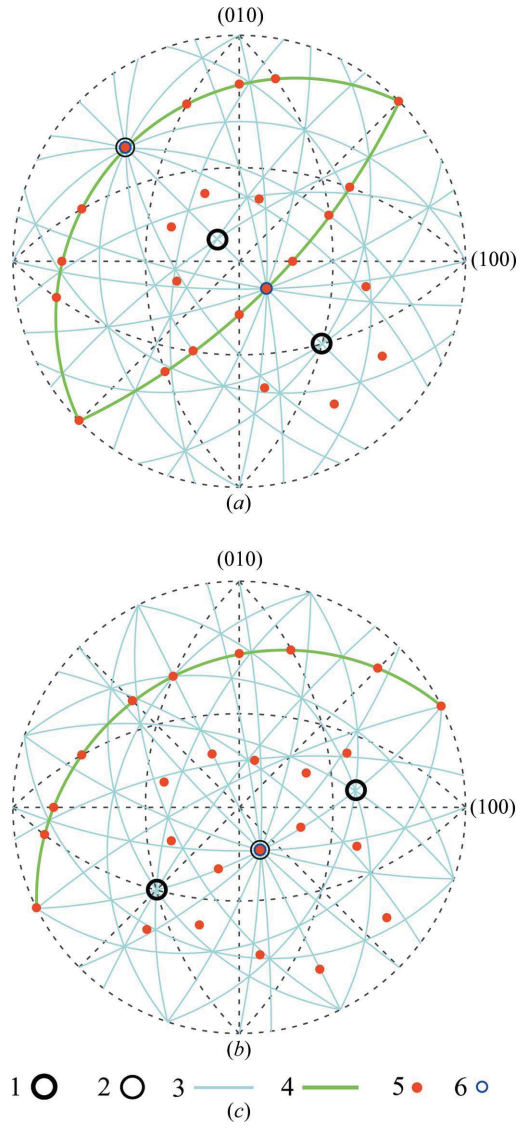

Figure 1
Stereographic projection of normals to the boundary planes for Σ9 (*a*) and Σ15 (*b*) misorientations. Circles 1 and 2 mark, respectively, the densest and the second-densest planes for *cF*-type lattices. The lines 3 and 4 mark tilt boundaries. Twist boundaries are marked by discs 4, and circles 6 indicate positions of poles of symmetric boundaries. The figure was drawn using the software *GBToolbox* (Glowinski & Morawiec, 2012).

Table 2
Top of auxiliary table with transposed Niggli-reduced bases, Niggli characters (Nc) and Bravais types (Bt) of CSLs for coincident *cF* lattices.

The last two columns indicate pairs of relevant vectors spanning the planes with the smallest areas per coincident node. See the supporting information for details.

Σ	Niggli-reduced basis	Nc	Bt	First	Second
3	$[\bar{1}\,0\,1 \mid 0\,1\,\bar{1} \mid \bar{2}\,\bar{2}\,\bar{2}]/2$	12	*hP*	(1)	(3)
5	$[2\,0\,0 \mid 1\,\bar{1}\,\bar{2} \mid 1\,\bar{2}\,1]/2$	18	*tI*	(1)	(2)
7	$[\bar{2}\,1\,\bar{1} \mid 1\,\bar{1}\,\bar{2} \mid \bar{1}\,\bar{2}\,1]/2$	4	*hR*	(1)	(4)
9	$[\bar{1}\,\bar{1}\,0 \mid 1\,\bar{2}\,\bar{3} \mid 2\,\bar{3}\,1]/2$	19	*oI*	(1)	(7)

Table 3
Most dense coinciding planes for *cF* lattices.

Symmetric interfaces are marked by 's' and twists are marked by 't'. The area per coinciding node is determined by Σ and β_{hkl}.

Σ	First-densest		β_{hkl}	Second-densest		β_{hkl}
3	$(1\,1\,1) \parallel (\bar{1}\,\bar{1}\,\bar{1})$	s	1	$(1\,\bar{2}\,1) \parallel (1\,1\,\bar{2})$	s	8
5	$(0\,\bar{2}\,1) \parallel (0\,1\,\bar{2})$	s	4	$(5\,3\,1) \parallel (\bar{5}\,\bar{3}\,1)$		7
7	$(\bar{3}\,\bar{5}\,1) \parallel (5\,3\,\bar{1})$		5	$(\bar{2}\,\bar{1}\,3) \parallel (3\,\bar{1}\,\bar{2})$	s	8
9	$(1\,\bar{1}\,1) \parallel (\bar{1}\,1\,\bar{5})$		3	$(\bar{2}\,2\,1) \parallel (2\,\bar{2}\,1)$	s	4
11	$(1\,\bar{1}\,3) \parallel (1\,\bar{1}\,\bar{3})$	s	1	$(\bar{3}\,3\,2) \parallel (3\,\bar{3}\,2)$	s	8
13*a*	$(0\,2\,3) \parallel (0\,\bar{3}\,\bar{2})$	s	4	$(0\,5\,1) \parallel (0\,\bar{5}\,1)$	s	8
13*b*	$(9\,3\,1) \parallel (\bar{9}\,1\,\bar{3})$		7	$(\bar{4}\,3\,1) \parallel (3\,\bar{4}\,1)$	s	8
15	$(\bar{1}\,\bar{1}\,1) \parallel (7\,1\,\bar{5})$		5	$(1\,\bar{2}\,5) \parallel (1\,\bar{2}\,\bar{5})$	s	8
17*a*	$(0\,4\,1) \parallel (0\,\bar{4}\,1)$	s	4	$(0\,\bar{5}\,3) \parallel (0\,3\,\bar{5})$	s	8
17*b*	$(1\,5\,5) \parallel (\bar{1}\,\bar{7}\,1)$		3	$(\bar{3}\,2\,2) \parallel (2\,\bar{3}\,2)$	s	4
19*a*	$(\bar{3}\,3\,1) \parallel (3\,\bar{3}\,1)$	s	1	$(1\,\bar{1}\,6) \parallel (1\,\bar{1}\,\bar{6})$	s	8
19*b*	$(\bar{5}\,3\,2) \parallel (3\,\bar{5}\,2)$	s	8	$(11\,1\,7) \parallel (\bar{7}\,\bar{1}\,11)$		9
21*a*	$(1\,1\,1) \parallel (\bar{1}\,\bar{1}\,\bar{1})$	t	7	$(\bar{4}\,\bar{1}\,5) \parallel (5\,\bar{1}\,4)$	s	8
21*b*	$(1\,\bar{4}\,2) \parallel (1\,2\,\bar{4})$	s	4	$(\bar{1}\,1\,1) \parallel (5\,\bar{1}\,\bar{1}\,1)$		7
23	$(3\,5\,9) \parallel (\bar{3}\,\bar{9}\,\bar{5})$		5	$(1\,\bar{6}\,3) \parallel (1\,3\,\bar{6})$	s	8
25*a*	$(0\,\bar{4}\,3) \parallel (0\,3\,\bar{4})$	s	4	$(0\,7\,1) \parallel (0\,\bar{7}\,1)$	s	8
25*b*	$(5\,1\,7) \parallel (\bar{1}\,\bar{5}\,\bar{7})$		3	$(\bar{5}\,4\,3) \parallel (4\,\bar{5}\,3)$	s	8
27*a*	$(1\,\bar{1}\,5) \parallel (1\,\bar{1}\,\bar{5})$	s	1	$(\bar{5}\,5\,2) \parallel (5\,\bar{5}\,2)$	s	8
27*b*	$(1\,\bar{2}\,7) \parallel (1\,\bar{2}\,\bar{7})$	s	8	$(\bar{5}\,1\,1) \parallel (5\,\bar{1}\,1)$	t	9
				$(1\,1\,1) \parallel (\bar{7}\,\bar{1}\,3\,\bar{5})$		9
29*a*	$(0\,5\,2) \parallel (0\,\bar{5}\,2)$	s	4	$(0\,3\,7) \parallel (0\,\bar{7}\,\bar{3})$	s	8
29*b*	$(\bar{4}\,3\,2) \parallel (3\,\bar{4}\,2)$	s	4	$(11\,\bar{1}\,9) \parallel (\bar{5}\,\bar{3}\,\bar{1}\,\bar{3})$		7
31*a*	$(1\,\bar{6}\,5) \parallel (1\,5\,\bar{6})$	s	8	$(13\,1\,5\,3) \parallel (\bar{1}\,\bar{5}\,\bar{1}\,\bar{3}\,\bar{3})$		13
31*b*	$(\bar{7}\,9\,5) \parallel (3\,\bar{1}\,\bar{1}\,5)$		5	$(2\,\bar{7}\,3) \parallel (2\,3\,\bar{7})$	s	8
33*a*	$(5\,\bar{5}\,7) \parallel (\bar{1}\,1\,\bar{3})$		3	$(\bar{4}\,4\,1) \parallel (4\,\bar{4}\,1)$	s	4
33*b*	$(3\,1\,1) \parallel (\bar{3}\,\bar{1}\,\bar{1})$	t	3	$(1\,\bar{7}\,4) \parallel (1\,4\,\bar{7})$	s	8
33*c*	$(7\,\bar{7}\,1) \parallel (\bar{1}\,1\,\bar{3})$		3	$(2\,\bar{2}\,5) \parallel (2\,\bar{2}\,\bar{5})$	s	4

2.7. Boundary types

For clarity, it is worth recapitulating the basics of grain boundary geometry. A boundary having a representation with the misorientation axis in the boundary plane is a tilt boundary, and a boundary having a representation with the misorientation axis perpendicular to the boundary plane is called a twist boundary. A boundary is symmetric if the boundary plane is a mirror between structures of the crystals. Symmetric boundaries exist only at some misorientations (Morawiec, 2012).

In the case of cubic lattices, most of the low-Σ CSLs allow for symmetric boundaries. With Σ < 50, only Σ39*b* does not belong to this class. If a boundary is a symmetry plane $(h\ k\ l)$,

the lattice misorientation is equivalent to the half-turn about $[h\ k\ l]$, the lattices have a common sublattice, and Σ is related to the coprime indices h, k and l via $\Sigma = (h^2 + k^2 + l^2)/\mathrm{GCD}(h^2 + k^2 + l^2, 2)$, where GCD denotes the greatest common divisor of its arguments. It is worth noting that some misorientations permit two nonequivalent symmetric boundaries. This is the property of $\Sigma3$, $\Sigma17b$ and the misorientations listed in Table 1 with the axes [1 0 0] and [1 1 0] (*i.e.* $\Sigma5$, 9, 11, 13*a*, 17*a*, 19*a*, 25*a*, 27*a*, 29*a*, 33*a* and 33*c*).

3. Results for cubic lattices

Results for low-Σ CSLs of *cF* and *cI* lattices are listed in this section, and those for *cP* lattices are in the supporting information. In all cases considered, the parameters of misorientations with $\Sigma \leq 33$ were fixed at values listed in Table 1. The area A_Σ of a planar cell is given in units of a^2 where a is the lattice parameter. The planar density of common nodes at the boundary plane is $1/A_\Sigma$.

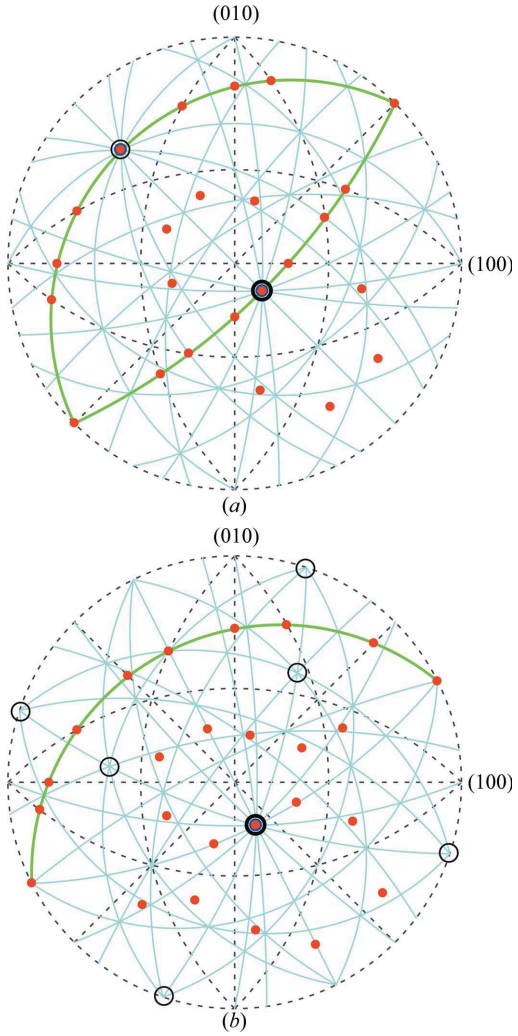

Figure 2
Stereographic projection of normals to the boundary planes for $\Sigma9$ (*a*) and $\Sigma15$ (*b*) misorientations with circles marking the densest and the second-densest planes for *cI*-type lattices. The legend is the same as in Fig. 1.

Intermediate results (the Niggli-reduced bases and the relevant vectors) are listed in auxiliary tables in the supporting information. These tables also contain byproducts of the procedure: the Niggli character and Bravais type of each CSL. For illustration, a part of such auxiliary data is shown in Table 2. The supporting information also contains a worked example of determination of dense planes for *cF* lattices related by $\Sigma15$.

Observations made below concern the data contained in Tables 3, 4 and the one with results for *cP* lattices. They have not been proven for CSLs of higher Σ. All listed CSL planes are multiple-tilt boundaries (*i.e.* the lattices are related by two or more rotations with distinct tilt axes). This fact is linked to the two-dimensional periodicity of the common lattice nodes.

3.1. *cF* lattices

The lattice planes of the densest and the second-densest interfaces with $\Sigma \leq 33$ are collected in Table 3. For the coinciding *cF* lattices, the area of the primitive cell of boundary planes is given by

$$A_\Sigma^{cF} = (\beta_{hkl}\,\Sigma)^{1/2}/4,$$

with the values β_{hkl} for particular planes listed in Table 3. For instance, the densest interface between f.c.c. crystals related by $\Sigma25a$ can be specified by the indices $(0\,\bar{4}\,3)$ in the first crystal and $(0\,3\,\bar{4})$ in the second crystal. It is a symmetric interface. With $\beta_{hkl} = 4$, the planar cell of common nodes has the area $A_\Sigma^{cF} = (5/2)a^2$. In the case of $\Sigma27b$, the second position is shared by two nonequivalent interfaces with the same planar densities. Most of the listed interfaces are symmetric. These interfaces can also be seen as twist boundaries. There are also cases of twist interfaces which are not symmetric. Positions of poles of the densest and the second-densest planes for $\Sigma9$ and $\Sigma15$ are shown on stereographic projections in Fig. 1.

3.2. *cI* lattices

The tables for coinciding *cI* lattices are arranged in the same way as those for *cF* lattices. The lattice planes of the densest and the second-densest boundaries are in Table 4. For the coinciding *cI* lattices, the area of the cell is

$$A_\Sigma^{cI} = (\beta_{hkl}\,\Sigma)^{1/2}/2.$$

Positions of poles of the densest and the second-densest planes for $\Sigma9$ and $\Sigma15$ are shown in Fig. 2.

The results for *cI* lattices are related to those for *cP* lattices. In both cases, if the CSL misorientation allows for symmetric boundaries, the densest interface is symmetric. Hence, if a CSL admits only one symmetric interface, it is the densest for both *cI* and *cP*. If there are two nonequivalent symmetric interfaces, they are exchanged, *i.e.* the one which is the densest for *cP* is the second dense for *cI* and vice versa.

3.3. Smith's formula

In a search for a method of determining dense boundary planes, Smith (1974) proposed a simple closed form expression for cell area per coinciding node,

Table 4
Most dense coinciding planes for *cI* lattices.

Σ	First-densest		β_{hkl}	Second-densest		β_{hkl}
3	$(1\bar{2}1) \parallel (11\bar{2})$	s	2	$(111) \parallel (\bar{1}\bar{1}\bar{1})$	s	4
5	$(031) \parallel (03\bar{1})$	s	2	$(0\bar{2}1) \parallel (01\bar{2})$	s	4
7	$(\bar{2}\bar{1}3) \parallel (3\bar{1}\bar{2})$	s	2	$(\bar{1}\bar{4}5) \parallel (41\bar{5})$		6
9	$(1\bar{1}4) \parallel (1\bar{1}\bar{4})$	s	2	$(\bar{2}\bar{2}1) \parallel (2\bar{2}1)$	s	4
11	$(\bar{3}32) \parallel (3\bar{3}2)$	s	2	$(1\bar{1}3) \parallel (1\bar{1}\bar{3})$	s	4
13*a*	$(051) \parallel (0\bar{5}1)$	s	2	$(023) \parallel (03\bar{2})$	s	4
13*b*	$(\bar{4}31) \parallel (3\bar{4}1)$	s	2	$(\bar{7}25) \parallel (7\bar{5}\bar{2})$		6
15	$(1\bar{2}5) \parallel (12\bar{5})$	s	2	$(\bar{3}10) \parallel (81\bar{5})$		6
				$(130) \parallel (\bar{4}\bar{7}5)$		6
17*a*	$(05\bar{3}) \parallel (03\bar{5})$	s	2	$(041) \parallel (0\bar{4}1)$	s	4
17*b*	$(433) \parallel (\bar{3}\bar{4}\bar{3})$	s	2	$(\bar{3}22) \parallel (2\bar{3}2)$	s	4
19*a*	$(1\bar{1}6) \parallel (1\bar{1}\bar{6})$	s	2	$(\bar{3}31) \parallel (3\bar{3}1)$	s	4
19*b*	$(\bar{5}32) \parallel (3\bar{5}2)$	s	2	$(\bar{1}\bar{7}8) \parallel (71\bar{8})$		6
21*a*	$(\bar{4}\bar{1}5) \parallel (5\bar{1}\bar{4})$	s	2	$(1\bar{2}3) \parallel (21\bar{3})$		6
21*b*	$(1\bar{4}2) \parallel (12\bar{4})$	s	4	$(3\bar{2}1) \parallel (11\bar{1}\bar{2})$		6
				$(132) \parallel (\bar{5}\bar{1}0\bar{1})$		6
				$(\bar{2}\bar{1}3) \parallel (2\bar{3}\bar{1})$		6
23	$(1\bar{6}3) \parallel (13\bar{6})$	s	2	$(\bar{5}\bar{7}8) \parallel (4\bar{1}\bar{1}\bar{1})$		6
25*a*	$(071) \parallel (0\bar{7}1)$	s	2	$(043) \parallel (03\bar{4})$	s	4
25*b*	$(\bar{5}43) \parallel (45\bar{3})$	s	2	$(\bar{1}\bar{0}\bar{7}1) \parallel (1152)$		6
27*a*	$(\bar{5}52) \parallel (5\bar{5}2)$	s	2	$(1\bar{1}5) \parallel (1\bar{1}\bar{5})$	s	4
27*b*	$(1\bar{2}7) \parallel (12\bar{7})$	s	2	$(411) \parallel (\bar{1}\bar{1}\bar{5}\bar{4})$		6
29*a*	$(037) \parallel (0\bar{7}\bar{3})$	s	2	$(052) \parallel (05\bar{2})$	s	4
29*b*	$(\bar{4}32) \parallel (3\bar{4}2)$	s	4	$(721\bar{1}) \parallel (\bar{2}\bar{7}\bar{1}\bar{1})$		6
				$(\bar{1}\bar{0}75) \parallel (132\bar{1})$		6
31*a*	$(1\bar{6}5) \parallel (15\bar{6})$	s	2	$(\bar{4}\bar{7}11) \parallel (74\bar{1}\bar{1})$		6
31*b*	$(2\bar{7}3) \parallel (23\bar{7})$	s	2	$(1314) \parallel (\bar{1}\bar{1}\bar{1}\bar{8})$		6
33*a*	$(1\bar{1}8) \parallel (1\bar{1}\bar{8})$	s	2	$(\bar{4}41) \parallel (4\bar{4}1)$	s	4
33*b*	$(1\bar{7}4) \parallel (14\bar{7})$	s	2	$(\bar{2}33) \parallel (5\bar{1}3\bar{2})$		6
33*c*	$(\bar{5}54) \parallel (55\bar{4})$	s	2	$(22\bar{5}) \parallel (2\bar{2}\bar{5})$	s	4

$$\sigma = \left(h^2 + k^2 + l^2\right)^{1/2}/\beta,$$

where β equals 2 for b.c.c. and 4 for f.c.c. structures. As presented by Smith (1974), the formula was believed to be applicable to a symmetric CSL boundary (*h k l*) when the misorientation of lattices is expressible as a 180° twist about [*h k l*]. It turns out that Smith's formula gives correct results only in some cases.

It is applicable to *cP* lattices with β = 1. If a CSL misorientation allows for symmetric boundaries, the densest interface is symmetric with cell area $A_\Sigma^{cP} = (\beta_{hkl}\Sigma)^{1/2}$ and β_{hkl} = GCD($h^2 + k^2 + l^2$, 2). Thus, $A_\Sigma^{cP} = \sigma$. If there are two symmetric boundaries, Smith's formula is applicable to both.

Smith's formula fails for some densest symmetric interfaces between *cI* lattices. Two such cases (Σ21*b* and Σ29*b*) are in Table 4 but more are visible in Fig. 3(*b*). If a CSL misorientation allows for symmetric boundaries, the densest interface is symmetric with β_{hkl} = 4/GCD($h^2 + k^2 + l^2$, 2). Hence, one has $A_\Sigma^{cI} = 2\sigma/\mathrm{GCD}(h^2 + k^2 + l^2, 2)$, *i.e.* A_Σ^{cI} is equal to σ if $h^2 + k^2 + l^2$ is even, and A_Σ^{cI} is equal to 2σ if $h^2 + k^2 + l^2$ is odd. In Fig. 3(*b*), Smith's formula corresponds to points on the lower branch described by $A_\Sigma^{cI} = (2\Sigma)^{1/2}/2$. It fails for the points in the upper branch described by $A_\Sigma^{cI} = (4\Sigma)^{1/2}/2$. (The outlier with β_{hkl} = 6 represents Σ39*b*.)

The case of coinciding *cF* lattices differs from *cP* and *cI* by the fact that the densest boundaries are not always symmetric. Even in the case of symmetric boundaries, Smith's formula fails in most *cF* cases. For symmetric boundaries listed in Table 3, the rule is that $A_\Sigma^{cF} = \sigma$ if all indices (*h k l*) are odd, and $A_\Sigma^{cF} = 2\sigma$ otherwise.

4. Generalization

A slightly modified version of the described scheme is applicable to exactly defined non-cubic latices related by $\Lambda' = R\Lambda$ and to common sublattices of distinct lattices. The latter case may be applicable to model some heterophase interfaces and orientation relationships.

Let Λ and Λ' be arbitrary three-dimensional lattices having a common three-dimensional sublattice. As above, let the matrices $[\mathbf{a}_i]$, $[\mathbf{a}'_i]$, $[\mathbf{a}_i^*]$ and $[\mathbf{a}_i'^*]$ contain basis vectors specified in an orthonormal reference frame for Λ, Λ', Λ^* and Λ'^*, respectively. The main complication is that the matrix $M = [\mathbf{a}_1^*\ \mathbf{a}_2^*\ \mathbf{a}_3^*\ \mathbf{a}_1'^*\ \mathbf{a}_2'^*\ \mathbf{a}_3'^*]$ is generally irrational. However, since the lattices are assumed to have a common three-dimensional sublattice, the matrix $[\mathbf{a}_i^*]^{-1}M = [\mathbf{a}_i]^{\mathrm{T}}M$ has rational entries and the rank of the matrix is 3. Now, let $[\mathbf{b}_i^*] = \mathrm{HR}(M)$ be the matrix built of the last three columns of $m^{-1}[\mathbf{a}_i^*]\,\mathrm{HNF}(m[\mathbf{a}_i^*]^{-1}M)$, where m is the least common multiple of denominators of entries of $[\mathbf{a}_i^*]^{-1}M$. As above, $[\mathbf{b}_i]$

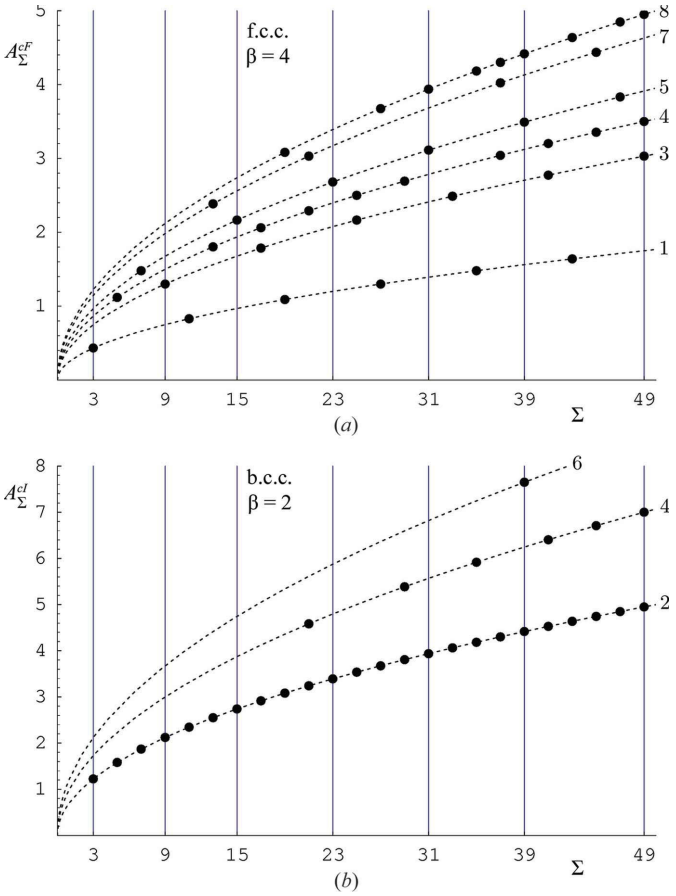

Figure 3
The area per coinciding node for the most dense boundary planes versus Σ for CSLs of *cF* (*a*) and *cI* (*b*) lattices. This is a corrected analog of Smith's figure (Smith, 1974). The dotted curves are $(\beta_{hkl}\Sigma)^{1/2}/\beta$, where β_{hkl} is the number ascribed to the curve.

reciprocal to $[\mathbf{b}_i^*]$ is a basis of the sublattice common to Λ and Λ'. The remaining steps of the procedure are the same as above with one exception: if the lattices are different, there is no ground for grain exchange symmetry, and only point symmetries need to be considered. The Miller indices of the plane perpendicular to a vector $\mathbf{v}$ are given by equation (1), or in terms of the matrices $[\mathbf{a}_i]$ and $[\mathbf{a}'_i]$, they are

$$(h\,k\,l) = (h_1\,h_2\,h_3) \propto \mathbf{v}^{\mathrm{T}}[\mathbf{a}_i] \text{ and } (h'\,k'\,l') = (h'_1\,h'_2\,h'_3) \propto \mathbf{v}^{\mathrm{T}}[\mathbf{a}'_i]$$

in the lattices Λ and Λ', respectively.

For a worked example of determination of the densest planes of intersecting distinct lattices, the reader is referred to the supporting information.

5. Final remarks

The density of coinciding sites in CSL-related crystals frequently arises in analyses of grain boundaries. Given two lattices, a method of determination of planes with high densities of coinciding lattice nodes was presented. It is applicable to arbitrary, possibly different, lattices having a three-dimensional common sublattice. The method relies on computing the Hermite normal form of an integer matrix and on Niggli reduction of the common sublattice. The procedure was applied to CSL-related cubic lattices, and the densest planes are listed for low-Σ lattice misorientations.

From a practical viewpoint, the key limitation of the described approach is that it is applicable to exact data. This does not affect the analysis of homophase interfaces between cubic lattices, but the limitation matters in the case of non-cubic lattices with parameters affected by experimental errors.

Acknowledgements

Appreciation is expressed to Gregory S. Rohrer for his comments on the manuscript.

References

Acton, A. F. & Bevis, M. (1971). *Acta Cryst.* A**27**, 175–179.
Brandon, D. G., Ralph, B., Ranganathan, S. & Wald, M. S. (1964). *Acta Metall.* **12**, 813–821.
Chalmers, B. & Gleiter, H. (1971). *Philos. Mag.* **23**, 1541–1546.
Cohen, H. (1993). *A Course in Computational Algebraic Number Theory*. Berlin: Springer.
Glowinski, K. & Morawiec, A. (2012). *Proceedings of the 1st International Conference on 3D Materials Science*, Seven Springs, PA, USA, edited by M. D. Graef, H. F. Poulsen, A. Lewis, J. Simmons & G. Spanos, pp. 119–124. Wiley.
Goodhew, P. J., Tan, T. Y. & Balluffi, R. W. (1978). *Acta Metall.* **26**, 557–567.
Gratias, D. & Portier, R. (1982). *J. Phys. Colloq.* **43**, C6-15–C6-24.
Křivý, I. & Gruber, B. (1976). *Acta Cryst.* A**32**, 297–298.
Morawiec, A. (2009). *J. Appl. Cryst.* **42**, 783–792.
Morawiec, A. (2012). *Z. Kristallogr.* **227**, 199–206.
Smith, D. A. (1974). *Scr. Metall.* **8**, 1197–1199.
Sutton, A. P. & Balluffi, R. W. (1987). *Acta Metall.* **35**, 2177–2201.
Wolf, D. (1992). *Materials Interfaces, Atomic-level Structure and Properties*, edited by D. Wolf & S. Yip, pp. 1–57. London: Chapman & Hall.
Wolff, P. M. de (2005). *International Tables for Crystallography*, Vol. A, edited by T. Hahn, pp. 750–755. Dordrecht: Springer.
Yang, Q. B. (1982). *Phys. Status Solidi A*, **72**, 343–351.